

# ELECTROCHEMICAL PROPERTIES OF Zr-V-Ni SYSTEM HYDROGEN STORAGE ALLOYS<sup>①</sup>

Yang Xiaoguang, Zhang Xiaobin, Shu Kangying, Lin Ganfu, Lei Yongquan and Wang Qidong

*Department of Materials Science and Engineering,  
Zhejiang University, Hangzhou 310027, P. R. China*

Zhang Wenkui

*Department of Applied Chemistry,  
Zhejiang University of Technology, Hangzhou 310014, P. R. China*

**ABSTRACT** The electrochemical properties of Zr-V-Ni system hydrogen storage alloys were investigated. In  $\text{ZrV}_{0.5}\text{Mn}_{0.3}\text{Ni}_{0.1}\text{Ti}_{0.1}$  ( $\text{T} = \text{Ni, Co, Fe, Al}$ ) system alloys, higher content of V and Mn (i. e.  $(\text{V} + \text{Mn})/\text{AB}_2 = 0.8$ ) brings forth more stable hydrides which have lower electrochemical capacities at room temperature. Meanwhile Al is a hydride-stabilizing element as well. The above alloys all have a capacity of about  $350 \text{ mAh} \cdot \text{g}^{-1}$  by raising temperature to 328 K. The substitution of Ti for Zr obviously alleviated their hydride thermodynamic stability for Zr-Ti-V-Ni system alloys. During charging/discharging process, the preferential anodic oxidation of component elements such as Ti and V will degrade the reversible hydrogen storage ability. The result was explained by the study of XRD, SEM observation and EDS analysis.

**Key words** Zr-V-Ni alloys alloying electrode performances

## 1 INTRODUCTION

In the binary alloys  $\text{ZrM}_2$  ( $\text{M} = \text{V, Cr or Mn}$  3d transition metal),  $\text{ZrV}_2$  mainly with a C15 Laves phase can absorb the highest hydrogen content, i. e.  $\sim \text{ZrV}_2\text{H}_6$  ( $\epsilon$  phase). The crystalline structures of  $\text{ZrV}_2\text{H}_x$  hydrides changed in the order of  $\beta$ ,  $\gamma$ ,  $\delta$  and  $\epsilon$  phases as the hydrogen concentration rose, which were all different from that of  $\text{ZrV}_2$  mother alloy. It was found that the hydriding enthalpies are very large in absolute value (i. e.  $\Delta H_{\text{plat}} = -79.5 \text{ kJ} \cdot \text{mol}^{-1}$  at  $x = 0.3 \sim 0.4$ ), accompanying with a much more steep hydrogen absorb/desorb pressure plateau. In order to adjust the stability and pressure plateau feature of  $\text{ZrV}_2\text{H}_x$  hydride, some work on alloying substitution, such as Ti for Zr and Ni for V, was reported recently<sup>[1-4]</sup>. The component elements Ti, V and so on were found to be irrevocably oxidized and dissolved in the working voltage range of  $-0.75 \text{ V} \sim -0.93$

V (vs  $\text{Hg}/\text{HgO}$ ), and their electrodes exhibited lower cycling stability.

In the present paper, the effect of alloying with Ti, Mn, Pd and Fe etc on the electrochemical properties of Zr-V-Ni system multicomponent alloys were investigated, and the results were explained in view of microstructure and EDS analyses.

## 2 EXPERIMENTAL

The ingots of Zr-V-Ni system alloys were prepared by arc-melting under Ar atmosphere and were re-melted 3 times to ensure homogeneity. The as-cast alloy ingots were mechanically crushed to particles of about 44  $\mu\text{m}$  for XRD analysis and for test electrode preparation as described previously<sup>[5]</sup>. For XRD analyses, Rigaku C-max-III B diffractometer with a  $\text{CuK}\alpha$  radiation and a nickel diffracted beam filter was used.

The hydride electrodes were prepared by

① Project 863-715-004-0060 supported by the National Advanced Materials Committee of China and Project 59601006 supported by the National Natural Science Foundation of China Received Oct. 28, 1997; accepted Feb. 27, 1998

cold pressing the mixtures of differently milled alloy powder and powdered electrolytic copper ( $44\mu\text{m}$ ) in a mass ratio of 1: 2 into copper holders to form porous pellets with 10 mm in diameter. Electrochemical charge-discharge tests were carried out in a tri-electrode electrolysis cell. The discharge capacities of hydride electrodes were determined by galvanostatic method. The electrodes were fully charged at a current density of  $100\text{mA}\cdot\text{g}^{-1}$  and cut-off potential set at  $-0.6\text{V}$  (vs  $\text{Hg}/\text{HgO}$ ).

The morphology of the hydride electrodes was observed by a HITACHI S-570 type Scanning Electron Microscopy (SEM). The distribution of components was analyzed by a PV 9900-PHILIPS type Energy Dispersive Spectrometer (EDS) as well.

### 3 RESULTS AND DISCUSSION

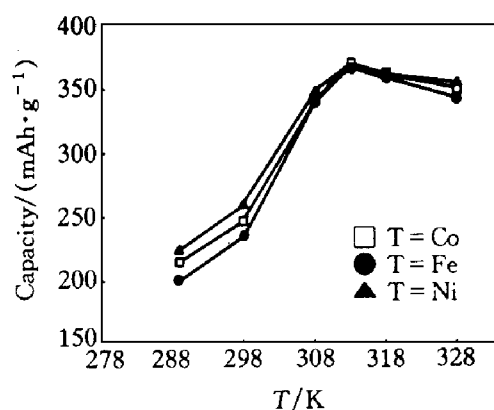
The electrochemical discharge capacities of the Zr-V-Ni multi-component hydrogen storage alloys were listed in Table 1. In the series of  $\text{ZrV}_{0.5}\text{Mn}_{0.3}\text{Ni}_{1.1}\text{T}_{0.1}$  ( $\text{T} = \text{Ni}, \text{Co}, \text{Fe}, \text{Al}$ ) alloys, the capacity decreases from 261 to 165  $\text{mAh}\cdot\text{g}^{-1}$  in the order of  $\text{Ni} > \text{Co} > \text{Fe} > \text{Al}$ . It is found that the substitution of Al for Ni lowers the capacity by about  $100\text{mAh}\cdot\text{g}^{-1}$ .

**Table 1** Discharge capacity of Zr-V-Ni multi-component hydrogen storage alloy (298 K)

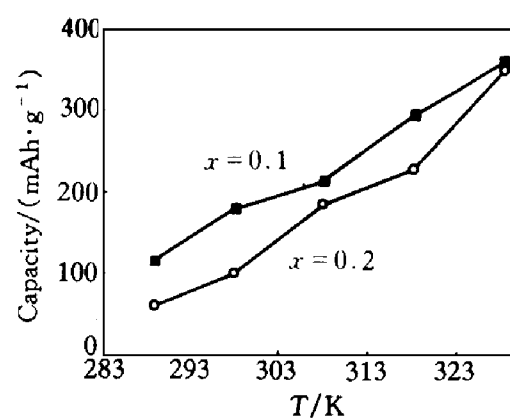
Alloy	Discharge capacity / $\text{mAh}\cdot\text{g}^{-1}$
$\text{ZrV}_{0.5}\text{Mn}_{0.3}\text{Ni}_{1.2}$	261
$\text{ZrV}_{0.5}\text{Mn}_{0.3}\text{Ni}_{1.1}\text{Co}_{0.1}$	249
$\text{ZrV}_{0.5}\text{Mn}_{0.3}\text{Ni}_{1.1}\text{Fe}_{0.1}$	237
$\text{ZrV}_{0.5}\text{Mn}_{0.3}\text{Ni}_{1.1}\text{Al}_{0.1}$	165
$\text{ZrV}_{0.5}\text{Mn}_{0.3}\text{Ni}_{1.1}\text{Al}_{0.2}$	110
$\text{Zr}_{0.8}\text{Ti}_{0.2}\text{V}_{0.6}\text{Mn}_{0.3}\text{Ni}_{0.9}\text{Fe}_{0.2}$	350
$\text{Zr}_{0.8}\text{Ti}_{0.2}\text{V}_{0.6}\text{Mn}_{0.3}\text{Pd}_{0.1}\text{Ni}_{0.8}\text{Fe}_{0.2}$	346
$\text{Zr}_{0.5}\text{Ti}_{0.5}\text{V}_{0.6}\text{Mn}_{0.2}\text{Pd}_{0.1}\text{Ni}_{0.8}\text{Fe}_{0.2}$	372

Fig. 1 shows the relation between the discharge capacity and the temperature of the  $\text{ZrV}_{0.5}\text{Mn}_{0.3}\text{Ni}_{1.1}\text{T}_{0.1}$  ( $\text{T} = \text{Fe}, \text{Co}, \text{Ni}$ ) series alloys. The discharge capacities all increased up

to  $350\text{mAh}\cdot\text{g}^{-1}$  as the temperature rises from 288 K to 315 K. It is found that the capacity changes little when Ni is replaced by the same fraction of Fe or Co. Nevertheless, the relation between the discharge capacity and temperature of  $\text{ZrV}_{0.5}\text{Mn}_{0.3}\text{Ni}_{1.1}\text{Al}_x$  ( $x = 0.1, 0.2$ ) series alloys is shown in Fig. 2. The discharge capacity of  $\text{ZrV}_{0.5}\text{Mn}_{0.3}\text{Ni}_{1.1}\text{Al}_{0.1}$  is about  $115\text{mAh}\cdot\text{g}^{-1}$  at 288 K, further more Al substitution ( $x = 0.2$ ) for Ni, it degrades to  $60\text{mAh}\cdot\text{g}^{-1}$  only. When the temperature rises up to 328 K, both electrodes exhibit a capacity of about  $355\text{mAh}\cdot\text{g}^{-1}$ .



**Fig. 1** Relation between discharge capacity and temperature of  $\text{ZrV}_{0.5}\text{Mn}_{0.3}\text{Ni}_{1.1}\text{T}_{0.1}$  ( $\text{T} = \text{Fe}, \text{Co}, \text{Ni}$ ) alloy



**Fig. 2** Relation between discharge capacity and temperature of  $\text{ZrV}_{0.5}\text{Mn}_{0.3}\text{Ni}_{1.1}\text{Al}_x$  ( $x = 0.1, 0.2$ ) alloys

From the experimental results, we might draw the following conclusion: the alloying degree (represented as  $(\text{V} + \text{Mn})/\text{AB}_2 = 0.8$ ) brings forth a too high stability for the hydride

to discharge capacity at ambient temperature in the  $\text{ZrV}_{0.5}\text{Mn}_{0.3}\text{Ni}_{1.1}\text{Ti}_x$  series alloys. It is necessary for them to lower the alloying degree ( $(\text{V} + \text{Mn})/\text{AB}_2$ ) to fulfil the promising capacity at room temperature; and the effect of Al substitution is different from those of Ni, Co or Fe VIII Group element. Al is regarded as a hydride-stabilizing element as Mn or V because of its stronger affinity to hydrogen atom.

Generally, the stability of hydride can be reduced by the Ti substitution for Zr. The discharge capacity of  $\text{Zr}_{0.8}\text{Ti}_{0.2}\text{Mn}_{0.3}\text{V}_{0.6}\text{Ni}_{0.9}\text{Fe}_{0.2}$  alloy is found to rise up to  $350 \text{ mAh} \cdot \text{g}^{-1}$  at room temperature. In the  $(\text{Zr}_{1-y}\text{Ti}_y)(\text{MnVPdNiFe})_2$  ( $y = 0.2, 0.5$ ) series alloys, when  $y = 0.2$ , its capacity is  $346 \text{ mAh} \cdot \text{g}^{-1}$ , when  $y = 0.5$  it is  $372 \text{ mAh} \cdot \text{g}^{-1}$ . However, their hydrogen storage concentrations are 2.46 and 2.49 H per formula respectively, on equal terms. Owing to the smaller atomic molar quantity of Ti than that of Zr, the mass specific discharge capacity was improved in the Ti-rich alloy in spite of the similar hydrogen storage density in mole fraction.

In order to study the effect of Pd slight alloying,  $\text{Zr}_{0.8}\text{Ti}_{0.2}\text{Mn}_{0.3}\text{V}_{0.6}\text{Pd}_x\text{Ni}_{0.8-x}\text{Fe}_{0.2}$  ( $x = 0$  and  $0.1$ ) alloys were designed on purpose. The capacities of  $\text{Zr}_{0.8}\text{Ti}_{0.2}\text{Mn}_{0.3}\text{V}_{0.6}\text{Pd}_{0.1}\text{Ni}_{0.8}\text{Fe}_{0.2}$  and  $\text{Zr}_{0.8}\text{Ti}_{0.2}\text{Mn}_{0.3}\text{V}_{0.6}\text{Ni}_{0.9}\text{Fe}_{0.2}$  are  $346$  and  $350 \text{ mAh} \cdot \text{g}^{-1}$ , respectively. There is no obvious difference. Low substitution of Pd for Ni induces little effect on the capacity and activation property in spite of the excellent electrochemical catalytic of Pd.

The cycling lifetime curves and activating processes of  $\text{Zr}_{0.5}\text{Ti}_{0.5}\text{V}_{0.6}\text{Mn}_{0.3}\text{Pd}_{0.1}\text{Ni}_{0.8}\text{Fe}_{0.2}$  and  $\text{Zr}_{0.8}\text{Ti}_{0.2}\text{V}_{0.6}\text{Mn}_{0.2}\text{Pd}_{0.1}\text{Ni}_{0.8}\text{Fe}_{0.2}$  are shown in Fig. 3. It is found that  $\text{Zr}_{0.5}\text{Ti}_{0.5}\text{V}_{0.6}\text{Mn}_{0.3}\text{Pd}_{0.1}\text{Ni}_{0.8}\text{Fe}_{0.2}$  electrode is easy to be activated owing to the rich Ti concentration. But its capacity decays severely with a residual capacity of less than  $200 \text{ mAh} \cdot \text{g}^{-1}$  after 200 cyclings. However, the capacity of  $\text{Zr}_{0.8}\text{Ti}_{0.2}\text{V}_{0.6}\text{Mn}_{0.2}\text{Pd}_{0.1}\text{Ni}_{0.8}\text{Fe}_{0.2}$  remains  $330 \text{ mAh} \cdot \text{g}^{-1}$  even after a 600 cycling test. Its capacity retention is as high as  $\sim 90\%$  at the same discharge depth. This result is similar to that in Zr-Cr-Ni system multicomponent alloy electrodes<sup>[6]</sup>. Higher Ti

substitution benefits to improve the maximum capacity and activation but degrades the cycling stability for Zr-V-Ni system alloys.

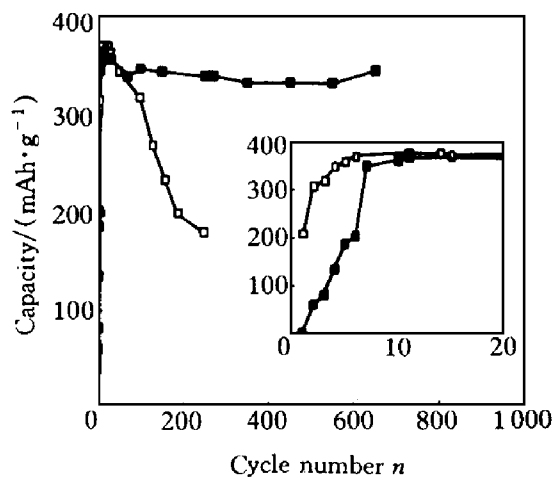


**Fig. 3** Cycling lifetime curves and activating processes of  $(\text{Zr}_{1-y}\text{Ti}_y)(\text{VMnPdNiFe})_2$  ( $y = 0.2, 0.5$ )  
 □ —  $\text{Zr}_{0.5}\text{Ti}_{0.5}\text{V}_{0.6}\text{Mn}_{0.3}\text{Pd}_{0.1}\text{Ni}_{0.8}\text{Fe}_{0.2}$ ;  
 ■ —  $\text{Zr}_{0.8}\text{Ti}_{0.2}\text{V}_{0.6}\text{Mn}_{0.2}\text{Pd}_{0.1}\text{Ni}_{0.8}\text{Fe}_{0.2}$

This phenomenon can be explained by the crystalline characteristics studies by XRD. The lattice parameter  $a$  of  $\text{Zr}_{0.5}\text{Ti}_{0.5}\text{V}_{0.6}\text{Mn}_{0.3}\text{Pd}_{0.1}\text{Ni}_{0.8}\text{Fe}_{0.2}$  alloy with an hcp structure changes from  $a = 0.4979 \text{ nm}$  in as-cast state to  $a = 0.4972 \text{ nm}$  after 10 cyclings, lattice parameter  $c$  expands from  $0.8134 \text{ nm}$  to  $0.8174 \text{ nm}$ ; After 200 cyclings of the corresponding alloy electrode, the value of  $a$  further reduces to  $0.4930 \text{ nm}$ , and parameter  $c$  increases to  $0.9343 \text{ nm}$ . The diffraction peaks were also found to broaden and their intensities lower obviously. As the cycling depth increases, the crystalline parameters change regularly. The interesting fact might imply that the component atoms occupying some certain crystalline positions selectively dissolve into the alkaline solution during the anodic polarization. This causes decay in electrochemical capacity of the studied alloys<sup>[7]</sup>.

Scanning electron microscopy (SEM) and X-ray dispersive spectrometry (EDS) were performed on the cycled  $\text{Zr}_{0.5}\text{Ti}_{0.5}\text{V}_{0.6}\text{Mn}_{0.3}\text{Pd}_{0.1}\text{Ni}_{0.8}\text{Fe}_{0.2}$  electrode. It was found that the component elements such as V, Ti, Mn and Ni are gradually oxidized and preferentially dissolved. The morphological aspects of the above alloy

$\text{Zr}_{0.5}\text{Ti}_{0.5}\text{V}_{0.6}\text{Mn}_{0.3}\text{Pd}_{0.1}\text{Ni}_{0.8}\text{Fe}_{0.2}$  after 10 and 200 cyclings were shown in Figs. 4(a) and (b) respectively. In Fig. 4(a) the electrode after 10 cyclings consists of alloy particles with a perfect shape. The article on A site in Fig. 4(a) is of a size of about 10  $\mu\text{m}$ , and the clear particle edge indicated little corrosion. On the B site in Fig. 4(a) there are a few small alloy particles with a size of 2  $\mu\text{m}$ . The EDS results on the A and B sites are listed in Table 2. The composition on A site can be calculated and rewritten as



**Fig. 4** SEM morphologies of  $\text{Zr}_{0.5}\text{Ti}_{0.5}\text{V}_{0.6}\text{Mn}_{0.3}\text{Pd}_{0.1}\text{Ni}_{0.8}\text{Fe}_{0.2}$  electrode  
(a) —10 cyclings; (b) —200 cyclings

$\text{Zr}_{0.5}\text{Ti}_{0.64}\text{Mn}_{0.19}\text{V}_{0.80}\text{Pd}_{0.09}\text{Ni}_{1.06}\text{Fe}_{0.255}$ , in which the concentration of V is higher than that of the original atomic ratio, on the contrary, Mn is lower. The concentration on B site is represented as  $\text{Zr}_{0.5}\text{Ti}_{1.26}\text{Mn}_{0.44}\text{V}_{1.84}\text{Pd}_{0.067}\text{Ni}_{2.65}\text{Fe}_{0.604}$ , the components (Ti, V and Ni) are richer than the designed composition except for Zr and Pd (maybe an oxide complex). The cycled electrode exhibits an obvious surface segregation. As shown in Fig. 4(b), after cycled for 200 times the alloy particles lost their sharp edges and are covered by an oxide layer, composition of which is designated as  $\text{Zr}_{0.5}\text{Ti}_{0.686}\text{Mn}_{0.23}\text{V}_{0.911}\text{Pd}_{0.095}\text{Ni}_{1.66}\text{Fe}_{0.336}$  by EDS analysis. The concentrations of Ti, V and Ni are all lower than that on B site in Fig. 4(a). The reasonable explanation is gradual dissolving of Ti, V and Ni into KOH solution<sup>[8]</sup>.

**Table 2** Atomic concentration on A and B sites in Fig. 4(a)

Site		Zr	Ti	V	Mn	Pd	Ni	Fe
A	Meas.	14.09	18.07	22.61	5.48	2.72	29.84	7.19
	Cal.	0.50	0.64	0.80	0.19	0.09	1.06	0.255
B	Meas.	6.80	17.07	25.02	5.98	0.91	35.98	8.22
	Cal.	0.50	1.26	1.84	0.44	0.067	2.65	0.604

## REFERENCES

- 1 Sawa H and Wakao S. *Denki Kagaku*, 1991, 58: 945.
- 2 Zuttel A, Meli F and Schlapbach L. *J Alloys Comp*, 1993, 200: 157.
- 3 Zuttel Z, Meli F and Schlapbach L. *J Alloys Comp*, 1994, 203: 235.
- 4 Huot J, Akiba E, Ogura T and Ishido Y. *J Alloys Comp*, 1995, 218: 101.
- 5 Yang X G, Lei Y Q, Wu J and Wang Q D. *Trans Nonferrous Metals Soc China*, 1995, 5(3): 61.
- 6 Yang X G, Lei Y Q, Chen Y L and Wang Q D. *Trans Nonferrous Metals Soc China*, 1997, 7(3): 1.
- 7 Yang X G, Lei Y Q, Zhang W K and Wang Q D. *Acta Metall Sinica*, (in Chinese), 1996, (8): 852.
- 8 Yan D Y, Sandrock G and Suda S. *J Alloys Comp*, 1994, 216: 237.

(Edited by peng Chaoqun)